NMR spin-echo measurements of reversible and irreversible motion of a driven vortex lattice

F. Lefloch,* W. G. Clark,† and W. H. Wong‡

Department of Physics and Astronomy, University of California at Los Angeles, Los Angeles, California 90095-1547

(Received 17 September 1998)

We report measurements of flux-line motion that is driven by a periodic rocking of the external magnetic field through a small angle in the type-II superconductor NbTi alloy filaments. The effect of the motion is to reduce the height of the ^{93}Nb NMR spin-echo signal. By investigating a broad range of parameters that characterize the rocking motion and the NMR pulse sequence, the scaling behavior discussed earlier [W. G. Clark, F. Lefloch, and W. H. Wong, Phys. Rev. B **52**, 7488 (1995)] is found to persist into a regime where irreversible flux-line motion causes an additional reduction of the echo height. The earlier model is extended phenomenologically to include irreversible displacements of the axis about which each vortex rocks. A second scaling relation for this mechanism that is seen experimentally is contained in the extended model. The results suggest that the irreversible part of the motion is driven by the rf pulse that forms the spin echo. [S0163-1829(99)08501-X]

I. INTRODUCTION

A substantial amount of work has been devoted to investigating the static and dynamic properties of flux lines (FL's) in several classes of superconductors: traditional current-carrying wires, high-temperature superconductors, organics, etc. Theoretical work has been applied to recently recognized (FL) phases, such as vortex glasses and liquids,[1–3] and various experimental tools have been used to investigate the properties of the FL structures, including electrical transport,[4,5] neutron diffraction,[6] magnetization,[7] μSr,[8] and NMR.[9] Much of the work shows that the dynamic and pinning properties of the FL's are rather complex.

NMR has played[10,11] and continues to play[12–15] a significant role in probing the static and dynamic properties of vortices in both conventional and high-T_c superconductors. One feature of interest is the response of a FL structure to a driving force. Several types of FL driving force are available: (1) a change in the magnitude of the applied magnetic field, (2) a change in its direction, or (3) a current perpendicular to the applied field. Such measurements probe the magnetic field distribution of flux-line lattice (FLL) and/or irreversible phenomena, and can be used for absolute measurements of the penetration depth λ in the volume of the sample.

In this paper, we present an NMR study of FL dynamics in multifilament NbTi wire that shows both a reversible and irreversible motion of the FL in response to a small periodic driving force. A preliminary report of this work[16] and analysis model[17] have shown that NMR spin echoes can be used as a sensitive local probe of driven FL motion. This model,[17] which calculates the reduction of the height of the NMR spin echo caused by driven FL motion in an isotropic, cylindrical type-II superconductor with the field perpendicular to the cylinder axis, is based upon a reversible motion of the FLL in response to rocking the magnetic field (or the sample) through a small angle; i.e., the FL throughout the sample follow the tipping of the externally applied magnetic field. It is also assumed that the point about which each FL rotates (''anchor point'') is the midpoint of each FL. One of its main features is that it predicts the experimentally observed[16] scal-

ing relation for the reduction of the spin-echo height in terms of the rocking angle amplitude (ψ_0), the rocking frequency (ω), and the spacing (τ) of the rf pulses used to generate the spin echo. Another useful aspect of the model is that for a known sample geometry and an applied magnetic field well below the upper critical field, the only adjustable parameter is λ. Because it requires a single adjustable parameter to fit the data, we refer to it as the one-parameter model. Thus, measurements of this kind can be used to obtain an absolute value of the penetration depth as a function of temperature.

In the next section, we present additional experimental results on NbTi multifilamentary wire that cover a substantially broader range of conditions than the earlier report.[16] They show that for ''moderate'' rocking of the field, the characteristics of the one-parameter model are retained. For more vigorous rocking the scaling relation is still followed, but there is an additional reduction of the spin-echo height that we attribute to a static displacement of the anchor point and a much smaller, irreversible motion of it during the rf pulse. Section IV contains a short review of the one-parameter model followed by a phenomenological extension which can account for our experimental observations. It is based upon a random, irreversible variation in time of the anchor point about which each FL rocks which we think is determined by the characteristics of the many pinning centers in the sample. This model also has the potential to characterize further irreversible effects that are related to the amplitude of the rf magnetic field used to generate the spin echoes.[18]

II. EXPERIMENTAL DETAILS AND RESULTS

Our NMR measurements of FL motion are based upon the following points. For a standard two-pulse spin-echo measurement in a static magnetic field, all nuclear spins contribute to the echo because the accumulated phase after the first pulse (dephasing period) is exactly canceled by the accumulated phase after the second pulse (rephasing period). However, when the FL's are driven by changing the direction of the external magnetic field, they move relative to the nuclei
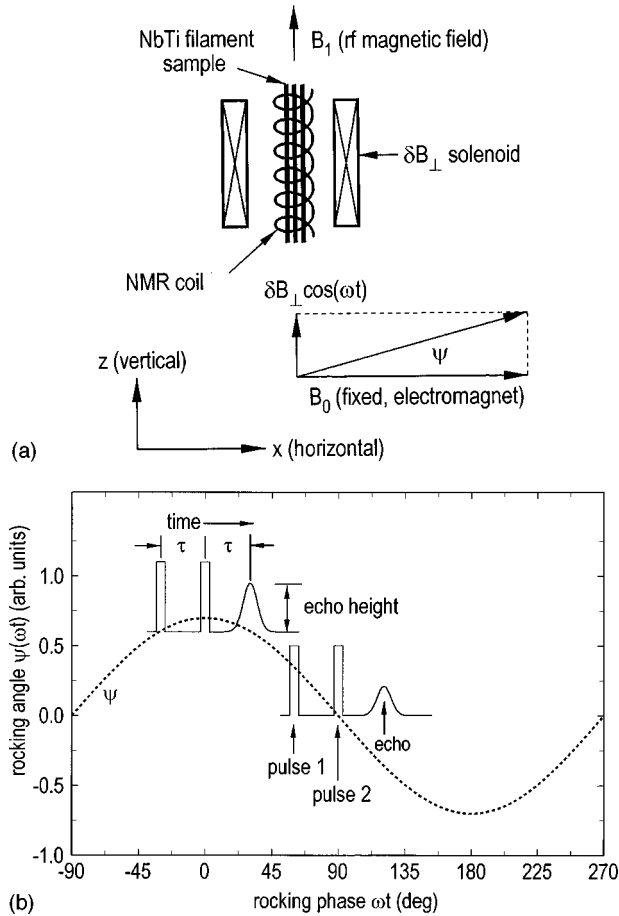
PRB <u>59</u>   7094

FIG. 1. (a) Orientation of the magnetic fields used in the experiments and (b) relation of the spin-echo timing to the rocking angle. The dotted line in (b) shows the variation of the rocking angle with time. The effect of FL motion on the spin echo is the reduction in height shown for the spin-echo sequence centered at $\omega t = 90°$ in comparison with the height at $\omega t = 90°$.

fixed in the sample and generate a corresponding time dependence of the local magnetic field. The consequence is that the accumulated phase of precession after the first pulse is not (except for unusual conditions) canceled by the accumulated phase after the second pulse, so that the height of the echo is reduced. Models of the vortex magnetic field and its motion are then used to relate the reduction in the spin-echo height to the details of the FL motion.

The sample used in this work is approximately 7000 NbTi filaments 10 μm in diameter and 1 cm long obtained by etching away the copper from commercial superconducting magnet wire (transition temperature $T_c \simeq 9$ K at zero field). Spin-echo signals were generated using a laboratory-built spectrometer and recorded on a digital scope connected to a computer. Low temperatures were obtained with a gas flow system in a standard ^{4}He cryostat. A diagram indicating the orientation of the sample and magnetic fields is shown in Fig. 1(a). The dc applied field of 1.16 T was provided by an electromagnet whose field was in a horizontal plane. An NMR coil was wound on the sample with its axis parallel to the filaments. For all of the measurements reported here, the axis of the NMR coil was along the vertical direction. An rf field amplitude $B_1 \simeq 10$ mT in the rotating frame was used for most of the measurements. The rocking field was induced

by a solenoid located in the dewar whose axis was also vertical. We measured the spin-echo response of the ^{93}Nb nuclei ($\gamma/2\pi = 10.407$ MHz/T and $I = \frac{9}{2}$) as a function of the parameters that characterize the rocking motion. Since the sample is an alloy with many imperfections, there is a large distribution of electric field gradients that causes a quadrupolar broadening of the ^{93}Nb signal on the order of 35 mT that obscures the line shape associated with the FLL in the superconducting state.

The main parameters that characterize the measurements are the angular amplitude of the rocking motion (ψ_0), its frequency (ω), the spin-echo pulse spacing (τ), and the applied magnetic field. In these experiments, ψ_0 was in the range 0.1–25 mrad (most values were below 6 mrad), $\omega/2\pi$ covered 10 to 400 Hz, τ was varied from 100 to 400 μs, and the external field was 1.16 T.

Figure 1(b) shows the timing relation between the phase of the rocking field and the spin-echo measurement for two different phases of the rocking field. The broken line shows the instantaneous value of ψ and the solid lines represent the occurrence of the two pulses (separated by τ) used for the spin-echo measurement. The upper one corresponds to a spin-echo measurement centered at zero rocking phase ($\omega\tau = 0$) and the one in the center of the figure a spin-echo measurement centered at $\omega\tau = 90°$. According to the model we use to interpret these experiments, when $\omega\tau = 0$, reversible driven motion of the flux-line lattice leads to no reduction of the spin-echo height. On the other hand, because the maximum flux-line lattice velocity occurs at $\omega\tau = 90°$, a spin-echo sequence centered about that value has the maximum echo height reduction.

In order to initiate each spin-echo measurement from the equilibrium nuclear magnetization, spin-echo measurements were made at a rate of about 1/sec, which is substantially less than the nuclear spin-lattice relaxation rate. Under these conditions, there were many field rocking cycles between successive NMR measurements.

There are several FL displacements that are significant for interpreting the results: (1) the maximum displacement of a FL during the (reversible) rocking motion, (2) the displacement of the FL during the spin-echo measurement, and (3) the irreversible change in the FL anchor point during the spin-echo measurement. For the model of reversible motion used to interpret our results[17] to be applicable, it is important that the FL displacement during the spin-echo measurement be small compared to the separation. Now we indicate some typical values for these characteristic displacements. At $\omega t = \pi/2$, the rocking angle traversed during the dephasing or rephasing time τ, is $\psi \simeq \psi_0 \omega\tau$ and the corresponding mean FL displacement for a cylinder during one dephasing/rephasing period is $\delta r \simeq (d/\sqrt{2})\psi_0\omega\tau$. For typical values of τ, ω, and ψ_0 ($\tau = 200$ μs, $\omega/2\pi \simeq 200$ Hz, and $\psi_0 = 3$ mrad), this displacement is $\delta r \simeq 2.5$ nm which is small compared to the flux-line lattice constant $a \sim 50$ nm at 1 T. The maximum amplitude of the FL displacement for these conditions at the surface of a 10 μm diameter wire is $0.5\psi_0 d \simeq 15$ nm. Because of the wide range of conditions used in our experiments, the actual values varied from much smaller to significantly larger than these typical values.

Another consideration is FL motion caused by the change in the *magnitude* of the magnetic field associated with the
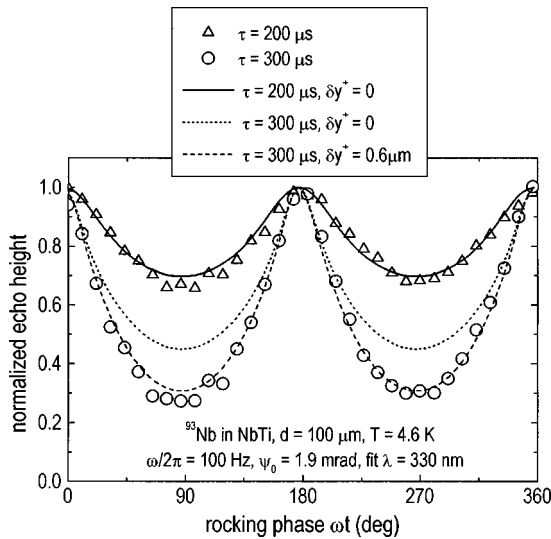
FIG. 2. Normalized ^{93}Nb spin-echo height as a function of the rocking phase at 4.6 K and an external field of 1.16 T in 10 μm diameter filaments of NbTi alloy for $\tau = 200$ and 300 μs, $\omega/2\pi = 100$ Hz, and $\psi_0 = 1.9$ mrad. The solid and dotted lines are the corresponding fits for the one-parameter model with $\lambda(4.6$ K$) = 330$ nm. The dashed line is the fit to the extended model with $\delta y^+ = 0.6$ μm.

FIG. 3. Normalized ^{93}Nb spin-echo height as a function of the rocking phase at 4.6 K and an external field of 1.16 T in 10 μm diameter filaments of NbTi alloy for $\psi_0 = 5.9$ and 11.7 mrad, $\tau = 100$ μs and $\omega/2\pi = 100$ Hz. The solid and dotted lines are the corresponding fits for the one-parameter model with $\lambda(4.6$ K$) = 330$ nm. The dashed line is the fit to the extended model with $\delta y^+ = 0.6$ μm.

rocking motion. It can cause FL motion by changing a via vortex nucleation or annihilation at the surface of the sample, followed by motion in and out of the sample. For the small values of ψ_0 used with our measurements, it is easily shown that the ratio of the FL displacement due to the change in the magnitude of the field to the displacement caused by the field rocking is $\frac{1}{4}\psi_0$, i.e., $<0.63\%$ for $\psi = 25$ mrad, the largest value we used. Thus, FL motion associated with a change in a is negligible in our experiments. In fact, we have chosen field rocking as the mechanism for driven FL motion because of the complexity of FL motion associated with a change in B. We expect, however, that spin-echo measurements of driven FL motion based upon changing B promise additional insight and surprises.

Figures 2–4 show typical experimental results for several values of these parameters. The symbols are experimental points and the curves are fits to the theoretical models discussed in the next section. It is evident that the spin-echo height is very sensitive to the external parameters and therefore to the motion of the flux lines.

There are several qualitative features to be compared with the model for reversible motion[17] of the FL outlined in the next section. First, it is seen that the echo height depends on the phase of the rocking angle. This phenomenon reflects the fact that for the conditions of these experiments the spin-echo amplitude is reduced when FL motion changes the local field during the spin-echo formation; the greater the velocity of FL motion the greater the reduction of the echo amplitude. The echo height is therefore a minimum when the rocking phase is $\pi/2$ and $3\pi/2$ (maximum FL velocity) and a maximum for 0, π and 2π (minimum FL velocity). It is also seen that the reduction in echo height at $\omega t = \pi/2$ is greater for the larger values of ψ_0, ω, and τ. An important implication of the normalized echo height returning to 1.0 is that within the resolution of the spin-echo measurements, the FL lattice mo-
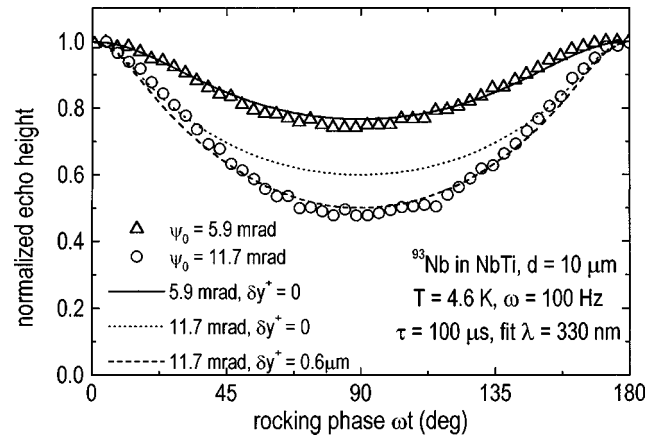
tion is reversible at $\omega t = 0$, π. For the data of Figs. 2 and 4, the maximum amplitude of the FL rocking motion varies from 0.5 to 9.5 nm and the maximum displacement during the spin-echo measurement is less than 0.4 nm. Thus, both of these quantities are quite small with respect to a. On the other hand, the data of Fig. 3 correspond to a maximum FL displacement amplitude of 58.5 nm and a maximum displacement during the spin-echo measurement of 3.7 nm. Thus, the former exceeds a but the latter is substantially less than a, as required by the model we use to interpret the results.

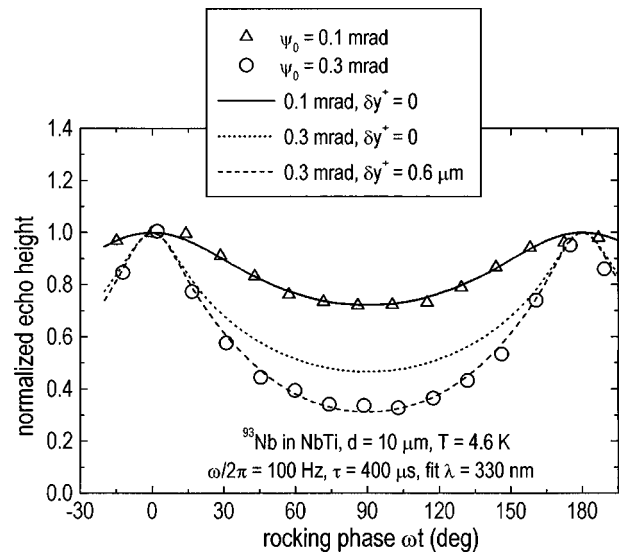In these experiments there is also a reduction in the echo

FIG. 4. Normalized ^{93}Nb spin-echo height as a function of the rocking phase at 4.6 K and an external field of 1.16 T in 10 μm diameter filaments of NbTi alloy for $\psi_0 = 5.9$ and 11.7 mrad, $\tau = 400$ μs and $\omega/2\pi = 100$ Hz. The solid and dotted lines are the corresponding fits for the one-parameter model with $\lambda(4.6$ K$) = 330$ nm. The dashed line is the fit to the extended model with $\delta y^+ = 0.6$ μm.
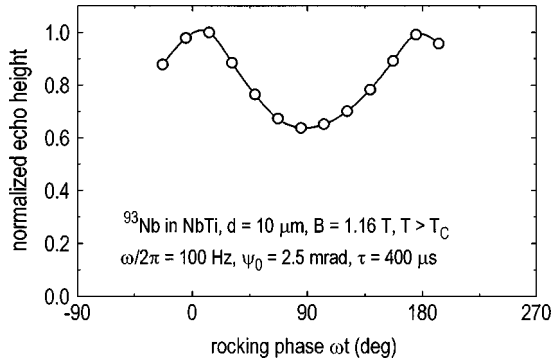
FIG. 5. Normalized ^{93}Nb spin-echo height as a function of the rocking phase at $T \simeq 12$ K $> T_c$ and an external field of 1.16 T in 10 μm diameter filaments of NbTi alloy in the normal state. This reduction in echo height is due to the quadrupolar interaction.

FIG. 6. Normalized ^{93}Nb spin-echo height as a function of the rocking phase at 4.6 K and an external field of 1.16 T in 10 μm diameter filaments of NbTi alloy for $\psi_0 = 25$ mrad, $\tau = 150$ μs, and $\omega/2\pi = 30$ Hz. The solid line is a guide to the eye. Irreversible motion of the vortices is responsible for the normalized echo height not returning to 1.0 for $\omega t = 90°$ and 270°.

height with field rocking that is not related to FL motion. It is a result of the quadrupolar interaction experienced by almost all of the ^{93}Nb nuclei in the alloy becoming time dependent when the externally applied field is rocked about the fixed sample. Furthermore, since there is a wide distribution of quadrupolar interactions caused by the polycrystalline character of the sample and the randomness of the alloy structure, the effect of field rocking on the quadrupolar contribution to the precession frequency differs for the various nuclei. A consequence is that the echo height is further reduced by the quadrupolar interaction. This effect is shown in Fig. 5, where the echo height as a function of the rocking angle is shown in the normal state, where no FL is present.

We have analyzed this effect in detail[19] and intend to publish the results elsewhere. It has similarities and differences in relation to the effect of field rocking on the echo when the FL is present in the superconducting state. The similarities are that this quadrupolar reduction in the echo height has the same dependence on ψ_0, ω, and τ as does the FL motion; i.e., it has the same functional dependence on the scaling variable ζ described in the next section. In particular, the quadrupolar reduction in echo height, which is measured in the normal state, is simply an additional factor that multiplies the reduction of the FL motion at the same value of ζ. In practice, this quadrupolar reduction (Fig. 5) is measured in the normal state and the corrected reduction due to FL motion is obtained by dividing the total reduction by the purely quadrupolar reduction.

There are also two ways in which the quadrupolar reduction in echo height differs from that of the FL motion: (1) The ratio of the strength of the quadrupolar and FL interactions varies with the sample, the material, and the nuclei investigated and (2) the quadrupolar effect does not depend on the sample dimensions, whereas the FL effect is very sensitive to them. If, as in our experiments, these differences are held constant, the multiplicative correction for the quadrupole effect described above can be used. It should also be noted that for all of the FL motion results presented in this paper, the parameters have been chosen to keep the quadrupole correction in the range 0–20 % of the combined quadrupolar and FL echo height reduction.

Finally, we point out that under some conditions the echo height does not return to 1.0 for $\omega t = 0$, π. One example is shown in Fig. 6, where the large value $\psi_0 = 25$ mrad is used.
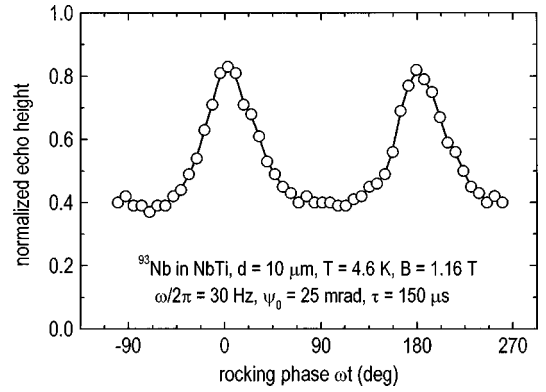
This reduction indicates that the driven FL motion did not follow the external rocking field. It is a manifestation of irreversible motion for which the phenomenological extension to the reversible case is developed in the next section.

III. MODELS AND THEIR APPLICATION TO THE EXPERIMENTS

The main focus of this section will be to compare our experimental results with models that describe how the echo height scales with the parameters of the field rocking experiment. First, we present an overview of the model for reversible FL motion developed earlier[17] and apply it to our measurements. Although it is adequate for some features of the experimental results, it fails to characterize others. We then extend the treatment to include a particular type of irreversible motion which does fit the data over a much wider range of conditions.

In the usual two-pulse spin-echo measurement, one starts from an equilibrium nuclear magnetization in the local magnetic field $\mathbf{B}(\tau)$ and applies a first pulse that tips the spins into a plane perpendicular to it. After that, each spin j precesses in its local field of magnitude $B_j(t)$ at the instantaneous angular frequency $\omega_j(t) = \gamma B_j(t)$, where t is the time and γ is the nuclear gyromagnetic ratio. After a duration τ a second rf pulse is applied that reverses the sense of precession and at $t = 2\tau$ a spin echo with a height $S_j(2\tau)$ is formed. The accumulated phase of the spin $\Phi_j(2\tau)$ due to a changing magnetic field $\Delta B_j(t)$, is

$$\Phi_j(2\tau) = \gamma \int_0^\tau \Delta B_j(t)dt - \gamma \int_\tau^{2\tau} \Delta B_j(t)dt \qquad (1)$$

and the total amplitude of the spin echo is

$$S_j(2\tau) = \sum_j e^{-(2\tau/T_{2j})} \cos[\Phi_j(2\tau)]$$

$$= S_0(2\tau) \sum_j \cos[\Phi_j(2\tau)], \qquad (2)$$

where T_{2j} is the spin-spin relaxation time (assumed here to be the same for all nuclei) and $S_0(2\tau)$ is the echo height in the absence of driven FL motion. The normalized spin-echo height is then defined as $S(2\tau)/S_0$. In this analysis, it is assumed that the local field $\mathbf{B}_j$ is parallel to the applied field $\mathbf{B}_0$, so that FL motion can affect the NMR precession rate, but that it does not contribute to spin-lattice relaxation, which requires a fluctuating component perpendicular to the static or slowly varying field that determines the instantaneous precession frequency.

When the local field does not change in time, as for a static FLL, the accumulated phase is zero and the normalized echo amplitude is equal to 1. The present model estimates the accumulated phase $\Phi_j(2\tau)$ for small sinusoidal displacement of the flux lines. To compare the model to experimental results we need to estimate the spin echo reduction in a cylindrical geometry. In the notation of Ref. 17, the rocking angle is

$$\psi(t) = \frac{\delta B_\perp}{B_0}\cos(\omega t) = \psi_0\cos(\omega t), \quad (3)$$

where B_0 and $\delta B_\perp$ are the amplitudes of the static and rocking fields, respectively.

We assume that the flux lines follow exactly the rocking of the external field by rotating at the frequency ω about their midpoint within the sample. They can, of course follow the external field direction by rotating about any point. The reason for assuming that they pivot about their midpoint in the sample is that this condition minimizes the dissipation associated with the corresponding flux flow. This constraint is relaxed in the extension of the model to irreversible motion that is considered later in this section.

In the limit of small displacements, the field variation induced by the coherent motion of the flux lines is

$$\Delta B_j(t) = (\boldsymbol{\nabla} B_j \cdot \mathbf{u}_j)y_s\psi_0\cos(\omega t), \quad (4)$$

where y_s is the distance to the axis of the filament and $\mathbf{u}_j$ is a unit vector collinear to the displacement, perpendicular to the direction of the flux lines and making an angle θ with the x direction of the FLL. By taking into account the density of nuclei $g(y_s)$ at the distance y_s and using Eqs. (1), (2), and (4) one obtains the normalized echo height

$$\frac{S(2\tau)}{S_0} = \frac{2}{N\pi}\int_0^\pi d\theta \sum_i \frac{1}{\zeta d G_j(\theta)} J_1[\zeta d G_j(\theta)], \quad (5)$$

where J_1 is the first order Bessel function of the first kind, d is the radius of a single filament, and

$$G_j(\theta) = \gamma(\boldsymbol{\nabla} B_j \cdot \mathbf{u}_j) = \gamma\left[\frac{\partial B_j}{\partial x}\cos\theta + \frac{\partial B_j}{\partial y}\sin\theta\right], \quad (6)$$

$$\zeta = \frac{4\psi_0}{\omega}\sin^2\left(\frac{\omega\tau}{2}\right)\sin(\omega t) = \zeta_0\sin(\omega t). \quad (7)$$

Note that $G_j(\theta)$ depends on the penetration depth and the coherence length through the derivatives of the local field B_j and that the average over θ accounts for the polycrystalline aspect of the FLL in the multifilamentary sample. For $B_0 \ll B_{c2}$, $G_j(\theta)$ is insensitive to ξ because $a \gg \xi$. Moreover,
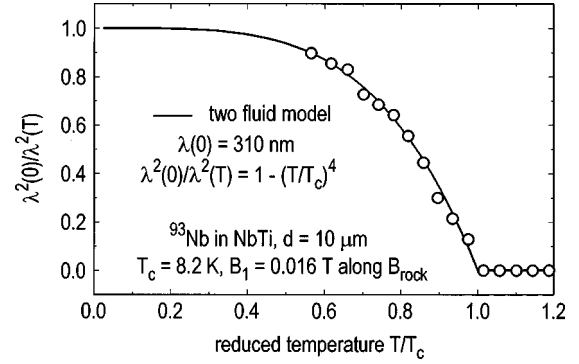

FIG. 7. Ratio $\lambda^2(0)/\lambda^2(T)$ as a function of reduced temperature for 10 μm diameter filaments of NbTi alloy obtained from measurements of the kind shown in Figs. 2–4. The solid line is a fit to the two-fluid model for the penetration depth.

the scaling variable ζ contains all the experimental parameters that are changed. To compare the model to the experimental results, we use Eq. (5) and compute the local field with the London model[20] in a unit cell of 50×50 points. The average over θ is obtained numerically. Equation (5) reveals some properties of the amplitude of the spin echo that can be checked experimentally. First, the echo height is a periodic function of the rocking phase ωt with a period half of that of the rocking field. Indeed, in this model, $S(2\tau)/S_0$ is 1 for $\omega t = 0, \pi$ and the minimum height, later referred as $S_{\min}$, occurs for $\omega t = \pi/2$. Second, the echo height depends on the external parameters τ, ω, and ψ_0 through the scaling variable ζ.

The solid and dotted lines in Figs. 2–4 show the fit of this model to the experimental results for various conditions at $T = 4.6$ K using $\lambda(T = 4.6 \text{ K}) = 330$ nm as the single adjustable fit parameter. Figure 2 shows the effect of varying τ and Figs. 3 and 4 display a broad combined range of τ and ψ_0. These conditions were chosen to provide a maximum reduction of 30% (triangles) and 50–70 % (circles). For the upper curves, where the reduction does not exceed 30%, the fit of the model (solid line) is rather good. On the other hand, the dotted line that shows the corresponding fit for the larger reductions models the reduction rather poorly. The extended model discussed below generates the dashed line that extends the good fit to the larger reductions. All of the reductions on Figs. 2–4 correspond to field rocking conditions that are ''gentle'' enough that the quadrupolar correction shown in Fig. 5 can be neglected.

The part of the curve of Figs. 2–4 that is most sensitive to the parameter λ is the echo height at $\omega t = 90°$. For measuring $\lambda(T)$, it is therefore easiest to choose this rocking phase and vary T. An example of such a measurement from a different run on the same material is shown in Fig. 7, where $\lambda(0)^2/\lambda^2(T)$ is plotted as a function of T. The solid line shows the behavior of the two-fluid model, for which $\lambda(0)^2/\lambda^2(T) = 1 - (T/T_c)^4$ with $\lambda(0) = 310\pm10$ nm. Again, the fit is rather good and the value for $\lambda(0)$ is close to the accepted value of 300 nm for a sample with $T_c = 9.5$ K at zero magnetic field.[21] This curve shows the ability of field rocking experiments to obtain absolute values of λ as a function of T. Examination of the model for the reduction of the echo height shows that it also has good promise for measuring the anisotropy of λ in anisotropic superconductors.
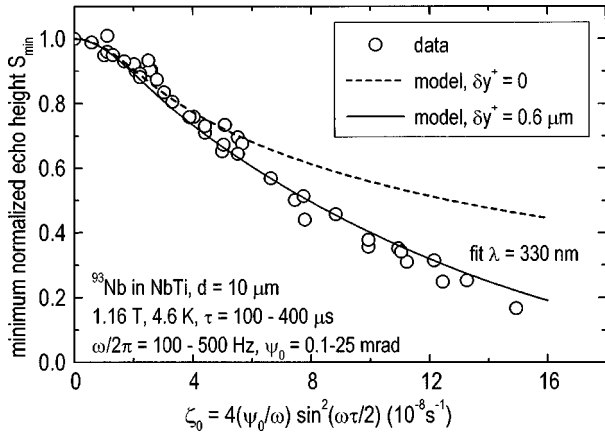
FIG. 8. Minimum Normalized ^{93}Nb spin-echo height ($\omega t = 90°$) as a function of the scaling variable for a broad range of ω, τ, and ψ_0. The data show that the scaling with ω, τ, and ψ_0 is followed up to $\zeta_0 = 16 \times 10^{-8}$ sec^{-1}. The dashed line, which is calculated with the one-parameter model fits the values of ζ_0 up to 4×10^{-8} sec^{-1}, but deviates significantly from the data above that. The solid line shows the fit obtained with the extended model over the entire range of ζ_0.

One of the major predictions of the model for the echo height reduction is the scaling behavior for ζ shown in Eqs. (5) and (7). Figure 8 shows a series of measurements of the echo height S_{min} (i.e., at $\omega t = \pi/2$) as a function of ζ_0 that includes a broad range of τ, ω, and ψ_0. The dashed line is the best fit for the smaller values of ζ_0 using Eq. (5). Two properties are clearly evident. First, the echo scales with ζ_0 over the entire range of the parameters τ, ω, and ψ_0. However, for $\zeta_0 \geq 5 \times 10^{-8}$ sec^{-1}, the measured echo reduction is greater than that predicted by the model of reversible motion. In what follows, we develop a phenomenological extension of this model for the echo height reduction that adds some irreversibility to the vortex motion. It is able to fit both the extension of the observed scaling behavior into the range of large ζ_0 and the reduction of the echo height at $\omega t = 0, \pi$ shown in Fig. 6, where a field rocking curve for a relatively large value of ψ_0 is shown. There, instead of returning to 1.0 at $\omega t = 0, \pi$, the normalized echo height reaches only 0.86.

In the above model, we considered only the periodic, reversible motion of the flux lines around their midpoint due to the relatively slow rocking of the external field. But the rf field, which in this experiment is applied in the same direction as the rocking field component, can also drive the vortices, but at the rf frequency. In effect, the rf field ''shakes'' the flux lattice in the same direction as the motion induced by the low frequency rocking. If this shaking induces the strained FLL to jump to a new pinning configuration, there will be a corresponding change in the local field that reduces the echo height, even at $\omega t = 0, \pi$. This kind of effect may explain the reduction of the echo height seen in Fig. 6. It also forms the basis for explaining effects we interpret as rf-assisted annealing of a strained FLL.[18]

As a guide to the kind of model needed to describe this reduction, we have examined a large number of measurements and found empirically that the reduction at $\omega t = 0, \pi$ scales according to the product $\psi_0 \tau$. This behavior is shown in Fig. 9, where S_{max} is graphed as a function of $\psi_0 \tau$ for several values of the rocking field parameters. There, it is
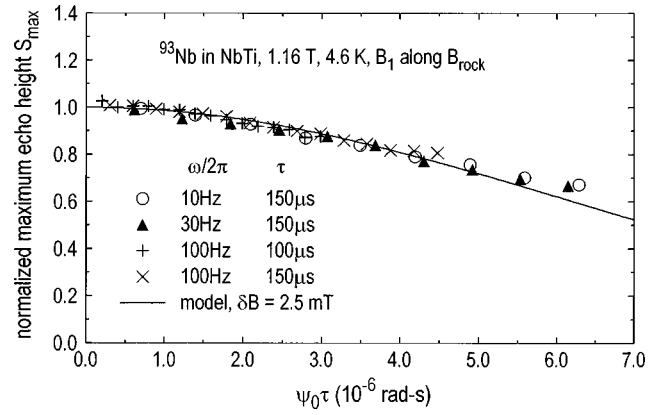

FIG. 9. Normalized ^{93}Nb maximum ($\omega t = 0°$) spin-echo height as a function of the product $\psi_0 \tau$ at 4.6 K and an external field of 1.16 T in 10 μm diameter filaments of NbTi alloy for different values of τ and $\omega/2\pi$. The rf magnetic field and the rocking field are both along the z direction. Scaling by $\psi_0 \tau$ is demonstrated by the overlap of the data and the solid line shows the fit obtained with the extended model described in the text.

seen that S_{max} does scale as $\psi_0 \tau$ for the range of parameters used in our measurements.

The extended range of scaling shown in Fig. 8 and the reduction of S_{max} seen in Fig. 9 can be fit to the simple, phenomenological extension of our previous model that we now describe. It involves two additional parameters introduced below. We shall refer to it as the three-parameter model. We emphasize that the introduction of these parameters is purely phenomenological. Although we believe they constitute a reasonable hypothesis, there is no detailed, microscopic theory to justify them that we are aware of.

First, it is assumed that the anchor point for the pth vortex, which is considered the one that dominates ∇B_j, is displaced by the distance δy_p from the midpoint ($y_s = 0$) of the filament and that δy_p is distributed randomly about zero for the different vortices. Moreover, we include a change in the anchor point that is induced by each rf pulse. In this way, the anchor point will not be the same during the dephasing and rephasing periods. Then, Eq. (4) becomes

$$\Delta B_{j1}(t) = \nabla B_j \cdot \mathbf{u}_j (y_s + \delta y_{p1}) \psi_0 \cos(\omega t) \qquad (8)$$

during the dephasing period and

$$\Delta B_{j2}(t) = \nabla B_j \cdot \mathbf{u}_j (y_s + \delta y_{p2}) \psi_0 \cos(\omega t) \qquad (9)$$

during the corresponding rephasing time.

Equation (1) is then replaced by

$$\Phi_j(t) = G_j(\theta)[\zeta(y_s + \delta y_p^+) + \delta y_p^- \sin(\omega \tau) \cos(\omega \tau)] \qquad (10)$$

with

$$\delta y_p^+ = \frac{\delta y_{p1} + \delta y_{p2}}{2}, \qquad (11)$$

$$\delta y_p^- = \frac{\delta y_{p1} - \delta y_{p2}}{2}. \qquad (12)$$

The quantities δy_p^+ and δy_p^- represent different aspects of the vortex rocking motion. The first, δy_p^+ is the average displacement of the anchor point of the vortex from the cylinder axis during the spin-echo measurement. A reasonable mechanism for it is the random location of pinning centers in the sample. If δy_{p1} and δy_{p2} are the same during the spin-echo measurement, the rocking motion is reversible and the anchor point is simply shifted from the cylinder axis. It is, therefore, difficult to discern from δy_p^+ if there is an irreversible component to the driven vortex motion. On the other hand, δy_p^- models the *change* in the anchor point induced by the second pulse of the spin-echo sequence. It reflects an irreversible aspect of the vortex motion. We believe it is a manifestation of the complex response of the pinned FLL to the ''shaking'' by the rf magnetic field.

If we assume $\delta y_p^- \ll \delta y_p^+$ and values of $\omega\tau$ that are not too small (justified later), the following expressions apply:

$$4(y_s + \delta y_p)\sin^2\left(\frac{\omega\tau}{2}\right) \gg \delta y_p^- \sin(\omega\tau), \qquad (13)$$

$$\Phi_j(t) = G_j(\theta)(y_s + \delta y_p^+)\zeta \quad \text{when} \quad \omega\tau = \pi/2, \qquad (14)$$

$$\Phi_j(t) = G_j(\theta)\delta y_p^- \frac{\psi_0}{\omega}\sin(\omega\tau) \quad \text{when} \quad \omega t = 0,\pi. \qquad (15)$$

These expressions are used to describe the scaling of $S_{\min}$ with ζ_0 for large values of ζ_0 and to describe the observed reduction in the normalized height of the echo to less than 1 at $\omega t = 0,\pi$ for large values of $G_j(\theta)\delta y_p^-(\psi_0/\omega)\sin(\omega\tau)$. The corresponding maximum reduction $S_{\min}$ is

$$S_{\min} = \frac{1}{N}\sum_j \int_0^d \frac{4}{\pi d}dy_s \sqrt{1 - \left(\frac{y_s}{d}\right)^2}$$
$$\times \int_0^\pi \frac{d\theta}{\pi}\cos[G_j(\theta)(y_s + \delta y_p^+)\zeta]. \qquad (16)$$

Integration over y_s gives

$$S_{\min} = \frac{1}{N}\sum_j \int_0^\pi \frac{d\theta}{\pi}\cos[G_j(\theta)\delta y_p^+\zeta]$$
$$\times \frac{1}{\zeta d G_j(\theta)}J_1[\zeta d G_j(\theta)]. \qquad (17)$$

One way to simplify Eq. (17) is to use

$$G_j(\theta)\delta y_p^+\zeta = \gamma\boldsymbol{\nabla}B_j\cdot\delta\mathbf{r}\frac{4}{\omega}\sin^2\left(\frac{\omega\tau}{2}\right)$$
$$= \gamma\Delta B_j\frac{4}{\omega}\sin^2\left(\frac{\omega\tau}{2}\right), \qquad (18)$$

where $\delta y_p^+\psi_0$ corresponds to the displacement $\delta\mathbf{r}$ of the flux line lattice that induces a change ΔB_j of the local field at the site of the jth nucleus. Since the distances δy_{p1} and δy_{p2} are random variables, the terms in Eq. (17) are evaluated using the probability distribution $P(\Delta B)$ for ΔB

$$S_{\min} = \int P(\Delta B)S_{\min}^{\text{rock}}\cos\left[\gamma\Delta B\frac{4}{\omega}\sin^2\left(\frac{\omega\tau}{2}\right)\right]d\Delta B, \qquad (19)$$

where $S_{\min}^{\text{rock}}$ is the maximum reduction of the spin-echo amplitude in the initial model [Eq. (5)]. The distribution $P(\Delta B)$ is modeled as a Gaussian with zero mean and second moment $(\delta B)^2$. With this assumption,

$$S_{\min} = S_{\min}^{\text{rock}}\exp\left\{-\frac{1}{2}\gamma^2(\delta B)^2\left[\frac{4}{\omega}\sin^2\left(\frac{\omega\tau}{2}\right)\right]^2\right\}. \qquad (20)$$

Then, $(\delta B)^2$ is expressed as

$$(\delta B)^2 \simeq (\nabla B)^2(\delta y^+)^2(\psi_0)^2, \qquad (21)$$

where $(\nabla B)^2$ is the mean square field gradient of the local field and $(\delta y^+)^2$ is the mean square of δy_p^+ for the distribution of vortices. Equation (20) then gives

$$S_{\min} = S_{\min}^{\text{rock}}\exp\left\{-\frac{1}{2}\gamma^2(\nabla B)^2(\delta y^+)^2\zeta^2\right\}. \qquad (22)$$

Equation (22) demonstrates that the echo height reduction at $\omega\tau = \pi/2$ associated with this three-parameter model for the flux motion multiplies the reduction associated with the reversible rocking motion and that it also has the same scaling variable ζ. Therefore, it has the potential to explain the extension of the scaling regime to $\zeta_0 > 5\times10^{-8}$ sec^{-1} seen in Fig. 8.

This result is applied to our data by using the London model with $\lambda(4.6\text{ K}) = 330$ nm and $\xi = 4$ nm at $B_0 = 1$ T to obtain $\sqrt{(\nabla B)^2} \approx 2.5\times10^5$ T/m. The solid line shows the application of this model for $\delta y^+ = 0.6$ μm. The same parameters provide the fit seen with the dashed (lowest) line on Figs. 2–4.

We now consider the reduction of the amplitude of the spin echo at $\omega t = 0,\pi$ for large values of ζ_0. As we have shown before, this amplitude ($S_{\max}$) is indeed a maximum, but it can be <1, which requires that the driven vortex motion includes an irreversible aspect. It is included in the three-parameter model via δy_p^- by using Eq. (15) for the accumulated phase and assuming that δy^- is a random variable with second moment $(\delta y^-)^2$. Then, $S_{\max}$ is given by

$$S_{\max} = \exp\left\{-\frac{1}{2}\gamma^2(\nabla B)^2(\delta y^-)^2\frac{\psi_0}{\omega}\sin\omega\tau\right\}$$
$$\simeq \exp\left\{-\frac{1}{2}\gamma^2(\nabla B)^2(\delta y^-)^2\psi_0\tau\right\}, \qquad (23)$$

where the lower row corresponds to the limit $\omega\tau \ll 1$, which almost always applies to our measurements. When this approximation applies, $S_{\max}$ is a function of the scaling variable $\psi_0\tau$. In Fig. 9 it is seen that this scaling relation is followed over a wide range of ψ_0 for two values of τ. The solid line is a fit of Eq. (23) using the value $\delta y^- = 10$ nm as the only additional adjustable parameter.

An important result of this analysis is that the three-parameter model, which includes irreversible driven vortex motion, covers both the scaling to $\zeta_0 = 16\times10^{-8}$ sec^{-1} for $S_{\min}$ and the reduction of $S_{\max}$. The values obtained for the location of the anchor points relative to the cylinder axis, $\delta y_{s1} \approx \delta y_{s2} \approx 0.5$ μm, appear reasonable for our sample geometry and justify the approximations that were made.

The ability of this model to fit the two scaling relations suggests the following microscopic picture. The term τ in the scaling relation of Fig. 8 [Eq. (23)] implies that at the maximum value of $\psi(t) = \psi_0$, the rf pulse moves the vortices, which then remain nearly fixed in position between pulses. If the irreversible motion were caused by the rocking forces acting alone, it can be shown that a higher power of τ should be observed. The appearance of the factor ψ_0 suggests that at the limit of the rocking motion the FLL is strained with respect to its optimal configuration relative to the pinning centers and that the displacement of the rocking anchor point by the rf field is proportional to this strain.

Although this three-parameter model appears to work well in this situation, it should be emphasized that λ (and therefore ∇B) can be obtained from measurements at the smaller values of ζ_0 that can be interpreted with the one-parameter model that does not require the introduction of the extra parameters δy^+ and δy^-. The work presented here is for a single value and direction of B_1. On the basis of exploratory measurements, we anticipate that the parameter δy^- will depend on both the magnitude and direction of B_1.

There are many candidates for future investigations that are related to the work described here. They include the extension to different polarization directions and amplitudes of the rf magnetic field, other sample geometries, such as a thin plate or film, anisotropic superconductors, where it should be possible to obtain the anisotropy of λ, high-temperature superconductors, with their multiplicity of fluxoid phases, materials with much weaker pinning than NbTi alloy, and alternative methods of driving the vortex structure, such as changing the field magnitude or applying an electrical current perpendicular to the magnetic field.

Another interesting possibility is to extend the method to measure the superconducting coherence length ξ. Measurements at fields much less than the upper critical field, such as those shown in Fig. 7, need only the single parameter λ to fit the data because the field distribution of only a tiny fraction of the sample is affected by ξ. As the upper critical field is approached, however, a progressively larger fraction of the sample has its local field determined by ξ. Under these conditions it is expected that values of both λ and ξ will be needed to model spin-echo measurements of driven vortex motion. Some preliminary modeling calculations we have done support this expectation.

IV. CONCLUSIONS

We have presented experimental results on the effects of reversible and irreversible small-amplitude driven FLL motion on the NMR spin-echo amplitude in the mixed state of a type-II superconductor with a cylindrical sample geometry. These measurements support the appropriateness of an elementary scaling variable ζ_0 which takes into account several of the experimental parameters that are used. It has been demonstrated that a single-parameter model of reversible motion[17] can be directly used for values of the scaling variable ζ_0 less than 5×10^{-8} sec^{-1}. In this range, the absolute value of the penetration depth λ can be obtained. For larger values of this scaling variable, the data can be fit to the three-parameter model developed here that includes irreversible driven motion of the vortices and a FL rotation anchor point that is not at the center of each FL.

*Present address: CEA-Grenoble, Département de Recherche Fondamentale sur la Matière Condensée, Service de Physique Statistique, Magnétisme et Supraconductivité, 17 Av. des Martyrs, 38054 Grenoble cedex 09, France.

†Author to whom correspondence should be addressed. Electronic address: wgclark@ucla.edu

‡Present address: Varian Associates, 3050 Hansen Way, Palo Alto, CA 94304-1000.

[1] M. V. Feigel'man, V. B. Geshkenbeim, and A. I. Larkin, Physica C **167**, 177 (1990).

[2] D. S. Fisher, M. P. A. Fisher, and D. A. Huse, Phys. Rev. B **43**, 130 (1991).

[3] G. Blatter, M. V. Feigel'man, V. B. Geschkenbein, A. I. Larkin, and V. M. Vinokur, Rev. Mod. Phys. **66**, 1125 (1994).

[4] S. Bhattacharya and M. J. Higgins, Phys. Rev. Lett. **70**, 2617 (1993).

[5] D. Dominguez, N. Gronbech-Jensen, and A. R. Bishop, Phys. Rev. Lett. **75**, 4670 (1995).

[6] U. Yaron, P. L. Gammel, D. A. Huse, R. N. Kleinman, C. S. Oglesby, E. Bucher, B. Batlogg, D. J. Bishop, K. Mortensen, K. Claussen, C. A. Bolle, and F. De La Cruz, Phys. Rev. Lett. **73**, 2748 (1994).

[7] L. Leylekian, M. Ocio, M. V. Feigel'man, and L. B. Ioffe, Physica C **235–240**, 2671 (1994).

[8] D. R. Harshman, R. N. Kleinman, M. Inui, G. P. Espinosa, D. B. Mitzi, A. Kapitulnik, T. Pfiz, and D. Ll. Williams, Phys. Rev. Lett. **67**, 3152 (1991).

[9] P. Carretta and M. Corti, Phys. Rev. Lett. **68**, 1236 (1992).

[10] P. Pincus, A. C. Gossard, V. Jaccarino, and J. H. Wernick, Phys. Lett. **13**, 21 (1964).

[11] J. M. Delrieu and J. M. Winter, Solid State Commun. **4**, 545 (1966).

[12] M. Mehring, F. Hentsch, Hj. Mattausch, and A. Simon, Solid State Commun. **75**, 753 (1990).

[13] P. Carretta, Phys. Rev. B **48**, 528 (1993).

[14] B. J. Suh, D. R. Torgeson, and F. Borsa, Phys. Rev. Lett. **71**, 3011 (1993).

[15] S. M. de Soto, C. P. Slichter, H. H. Wang, U. Geiser, and J. M. Williams, Phys. Rev. Lett. **70**, 2956 (1993).

[16] W. G. Clark, W. H. Wong, and F. Lefloch, Physica C **235–240**, 1793 (1994).

[17] W. G. Clark, F. Lefloch, and W. H. Wong, Phys. Rev. B **52**, 7488 (1995).

[18] W. G. Clark, F. Lefloch, and W. H. Wong (unpublished).

[19] W. G. Clark, F. Lefloch, and W. H. Wong (unpublished).

[20] E. H. Brandt, J. Low Temp. Phys. **76**, 355 (1988).

[21] R. J. Donnelly, in *Physics Vade Mecum*, edited by H. L. Anderson (American Institute of Physics, New York, 1981), p. 121.